

Risk perception in epidemic modeling

Franco Bagnoli*

Department of Energy, University of Florence, Via S. Marta, 3 I-50139 Firenze, Italy and CSDC and INFN, sez. Firenze

Pietro Liò

Computer Laboratory, University of Cambridge, JJ Thompson Avenue, CB30FD Cambridge, United Kingdom

Luca Sguanci

Centro per lo Studio di Dinamiche Complesse (CSDC), University of Florence, Via G. Sansone 1, Sesto Fiorentino (FI)

(Received 15 May 2007; revised manuscript received 23 August 2007; published 5 December 2007)

We investigate the effects of risk perception in a simple model of epidemic spreading. We assume that the perception of the risk of being infected depends on the fraction of neighbors that are ill. The effect of this factor is to decrease the infectivity, that therefore becomes a dynamical component of the model. We study the problem in the mean-field approximation and by numerical simulations for regular, random, and scale-free networks. We show that for homogeneous and random networks, there is always a value of perception that stops the epidemics. In the “worst-case” scenario of a scale-free network with diverging input connectivity, a linear perception cannot stop the epidemics; however, we show that a nonlinear increase of the perception risk may lead to the extinction of the disease. This transition is discontinuous, and is not predicted by the mean-field analysis.

DOI: [10.1103/PhysRevE.76.061904](https://doi.org/10.1103/PhysRevE.76.061904)

PACS number(s): 87.23.Ge, 05.70.Fh, 64.60.Ak, 89.75.Hc

I. INTRODUCTION

In spring 2006, the potential threat of bird flu dominated headlines in U.K. newspapers. On March 26, 2006, *The Sun* has called it “the day we all dreaded,” while *The Guardian* says avian flu is “almost certain to spread to wild birds across the U.K.” *The Daily Telegraph* adds that the most likely human victims will be poultry farmers, who will be bankrupted. But *The Mirror* calls for calm, saying people have a better chance of winning the lottery than catching the virus. Interestingly, given a certain amount of clustering of wealthy residents and a correlation between wealth and readers preference, this would translate into a differently informed neighborhood. When the epidemic is over its peak or other news has just peaked or media has “cried wolf” too many times over unfounded health scares, there is a quick drop in attention to that disease (something similar is reported nowadays for HIV). In other parts of the world, for example, Indonesia—a country with 18 000 islands—people reacted differently to the bird flu epidemics. Despite awareness campaigns in the media and even door-to-door visits in some of the islands, many Indonesians remained oblivious to the dangers of being in contact with diseased birds, and aware of the need to inform the authorities and implement a cull. Note that awareness campaigns, such as during the SARS epidemics, are expensive and may result in culling, and reductions in commerce, travel, and tourism. The media hype over epidemics threats has a close similarity in how worried or fatalist, resilient, skeptical, or cheeky may be ones friends and neighborhood. Therefore, the individual perception of the risk of becoming infected is a key factor influencing the spread of an epidemic and, toward a realistic infer-

ence, epidemiological models should incorporate such a parameter [1].

In order to investigate the effect of risk perception in influencing the spread of a disease, let us start from simple, yet meaningful models, such as the susceptible-infected-susceptible (SIS) or susceptible-infected-removed (SIR) models. These models are defined on a network where individuals, or groups of individuals, correspond to the nodes and links representing social contacts and relationships among them. Most classical studies used either a regular lattice or a random one. Both of those choices are characterized by a well defined value of the mean connectivity $\langle k \rangle$, and small variance $\langle k^2 \rangle - \langle k \rangle^2$. As shown by Watts and Strogatz [2], the simple rewiring of a small fraction of links in an otherwise regular lattice results in a sudden lowering of the diameter of the graph, without affecting the average connectivity or the degree of clustering. This *small world* effect manifests itself in a dramatic shortage of the distance between any two individuals, almost without affecting the local perception of the network of contacts. The consequences of epidemics spreading are important: just a few long-distance connections may promote the spread of a disease in rural areas, whereby an epidemic would otherwise diffuse very slowly.

However, the investigations of social networks have shown that they are quite different from regular and random graphs [3,4]. The probability distribution of contacts often exhibits a power-law behavior [$P(k) \propto k^{-\gamma}$], with an exponent γ between 2 and 3 [5,6]. This distribution is characterized by a relatively large number of highly connected hubs, which are presumably responsible for the spread of epidemics. Moreover, such distributions have a diverging second moment $\langle k^2 \rangle$ for $\gamma \leq 3$ and a diverging average connectivity $\langle k \rangle$ for $\gamma \leq 2$.

The influence of the connectivity on the spreading dynamics is well outlined by a simple mean-field analysis. Let us

*franco.bagnoli@unifi.it

consider for the moment a tree with fixed connectivity k . In a SIS model with immediate recovery dynamics, a single infected individual may infect up to k neighbors [7], each one with probability τ . The temporal behavior of the mean fraction c of infected individuals is given by

$$c' = \sum_{s=1}^k \binom{k}{s} c^s (1-c)^{k-s} [1 - (1-\tau)^s], \quad (1)$$

where $c \equiv c(t)$, $c' \equiv c(t+1)$, and the sum runs over the number s of infected individuals. The basic reproductive ratio R_0 [8] is simply given by $R_0 = k\tau$, so that the epidemic threshold $R_0 = 1$ corresponds to $\tau_c = 1/k$. This means that for a fixed connectivity, only diseases with an infectivity of less than $1/k$ do not spread.

In heterogeneous networks (nodes with different connectivity) the mean-field analysis, reported in Sec. III, gives $\tau_c = \langle k^2 \rangle / \langle k \rangle$. In the case $\langle k^2 \rangle \approx \langle k \rangle^2$, τ_c is again equal to $1/\langle k \rangle$.

In summary, the result is that in very nonhomogeneous networks, with diverging second moment $\langle k^2 \rangle$ (and even worse in those with diverging average connectivity $\langle k \rangle$), a disease will always spread regardless of its intrinsic morbidity [9].

This result can be modified by the assortativity degree of the network and by the presence of loops, not considered in the mean-field analysis. In networks with assortative connections (hubs are preferentially connected to other hubs), it may happen that epidemics spread for any finite infectivity even when the second moment is not diverging [10,11], while for disassortative networks the reverse is true; epidemics may be stopped by lowering the infectivity with random vaccination campaigns, even in the presence of a diverging second moment [10]. This is particularly evident in networks lacking the small-world property (a consequence of high disassortativity) [12,13].

In small-world networks with a diverging second moment, it is quite difficult to stop an epidemic. The most common recipes are vaccination campaigns (removal of nodes) or modification of the social structure (removal of links), which mathematically corresponds to site and bond percolation problems. To be efficient, a vaccination campaign must be targeted to hubs, either directly [3] or implicitly, for instance, by exploiting the fact that hubs are the most probable neighbors of many nodes [14].

The modification of the social structure can be obtained by coercive methods (quarantine, etc.) or by raising alerts so as to modify traveling and business patterns, but this option may be so expensive that the amount of money put into restoring the previous situation may exceed that used to cure ill people [15].

However, epidemics in the modern world are relatively uncommon, and most of them are stopped quite easily in spite of the presence of high network connectivity. The existence of an epidemic threshold on such networks has motivated the investigation of the effects of connectivity-dependent infectivity [16–18]. In this latter case, most of the investigations have been performed using mean-field techniques, thus disregarding the presence of loops.

Loops are irrelevant at and near the percolation threshold [19], and therefore one can treat the network as a tree in these conditions. However, for processes evolving on percolating networks, this assumption may not hold.

At present, the basic models used do not take into consideration the *knowledge* that all human beings have nowadays about the mechanisms of diffusion of diseases. In fact, even in the absence of vaccination campaigns, a disease that manifests itself in a visible way induces modifications in the social network: lower frequency of contacts (usage of mass transportation systems), higher level of personal hygiene, prevention measures (masks), etc. Indeed, recent works stress the importance of using a time-dependent bare infectivity to reproduce real patterns of epidemics [20–23].

Viruses with high mutation rates (like computer viruses) follow a dynamics which is more similar to SIS than to SIR [24], even in the presence of immunization. On the other hand, the origin of vaccinations comes from cross immunity conferred by strains with lower pathogenicity.

We shall study here a SIS model in which the bare infectivity of the spreading agent is modulated by a term that tries to model the effects of the perception of the risk of being infected.

We assume that this perception is just an increasing function of the fraction of ill people in the neighborhood, given that the illness presents visible symptoms. This assumption is modeled after the heuristic-systematic information-processing model [25] that simply states that attitudes are formed and modified as people gain information about a process. In the absence of explicit alarm or communication, the only way of gaining this information is through examination of people in the neighborhood. Individuals can process information in two ways: either heuristically, using simple semi-unconscious schemes, or carefully examining them in a rational way, also called data driven and schema driven, respectively.

It states that the processing of information can follow two paths: a slow and conscious one, or a faster and unconscious one, which in general emerges from training. For instance, driving a car, after proper training, becomes an automatic process. Education and daily experiences also contribute to training, which is moreover favored for certain topics (say, recognition of social role, aggression, etc.) by the structure of our brain, as a result of natural selection. The unconscious mechanism is generally monitored, so that an exceptional event such as, for instance, the vision of something unusual during driving, may pass control to the conscious part of the brain.

The unconscious mechanism is rather schematic, and is exploited by advertisements based, for instance, on fear or sex. Experience says that the efficacy of an advertisement based on some risk is proportional to the perception of the risk, with a lower threshold for low perceived risks and an upper threshold for *shocking* risks. In the case of too high risk, there is a removal mechanism that makes them unusable for advertisement. This effect is a common experience in all campaigns about prevention: it is very difficult to make campaigns against risks that are perceived to be low (such as driving, smoking, drinking, etc.). One has to first rise the perception of the risk. On the other hand, a too high risk (like

advertisements on cancer risk for smoking tobacco) is equally useless since it is not perceived.

Notice that the perception of a risk may have no connection with the actual value of the risk. An example of this is the perceived risk of driving with respect to the risk of taking an airplane.

In this work we simply assume that the local information (not enhanced by alarms) about the incidence of the illness translates into a lowering of the infection probability, implementing only the “linear part” of the information-processing model. In principle, it is possible to compare the effective susceptibility to infection for diseases that manifest themselves in a visible and in an invisible way and test experimentally this hypothesis. In summary, we assume that (1) the illness is visible prior to or at the same moment it becomes infective; (2) the perception of the risk of being infected is proportional to the fraction of contacts with ill people, with respect to the total number of contacts; and (3) all individuals have the same perception and reaction, independently from their culture, role, etc. (uniform society). This last point is introduced because we are interested in the influence of the dishomogeneity of contacts, and we do not want to mix another source of differences among individuals.

Notice that the actual relation between risk and the perception of risk is of no importance, as long as all individuals share the same parameters and it is always within the low and high threshold of the heuristic-systematic model.

In our model, the infectivity is a dynamical quantity. Although the idea of modulating the infectivity of the infection process is not new, it is generally studied (mostly in the mean-field approximation) as a function of time [20–23] and/or of connectivity [16,17], depending on the total infection level [26,27]. In this latter approach, a nonlinear growing dependence of the infection rate on the total number of infected people may originate bifurcation and chaotic oscillations.

As we shall show in the following, mean-field analysis [28] may not capture the essential phenomena in highly connected networks. Moreover, we study the case of a decreasing infection rate with an increasing local infection level, which might also induce chaotic oscillations at the mean-field level (see Ref. [29] and Sec. II). However, one should consider that chaotic oscillations on networks easily desynchronize, and the resulting “microscopic chaos” is quite different from the synchronous oscillations predicted by mean-field analysis [30], which may nevertheless be observed in lattice models in the presence of long-range coupling [31].

We explicitly describe the model in Sec. II, analyze it using mean-field techniques in Sec. III, and study numerically its behavior on different types of networks in Sec. IV. Conclusions and perspectives are drawn in Sec. V.

II. MODEL

In this paper we study the dynamics of an infection spreading over a network of N individuals. We use different kinds of networks: regular, with long-range rewiring [2], random, and scale-free [5]. The network structure is considered not to depend on the infection level.

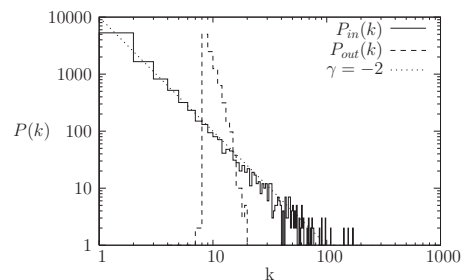


FIG. 1. Distribution of input and output connections for the scale-free network used in simulations.

Let us denote by $P(k)$ the probability distribution of connectivity k . We shall denote by $z = \mu_1(P)$ the average connectivity (first moment of the distribution) $z = \langle k \rangle = \sum_k k P(k)$, and by μ_2 , $\mu_2 = z^2$. The rewiring of the network is performed by starting from a regular lattice in one dimension, detaching a fraction p of links from one end and attaching them to randomly chosen nodes. The regular case is studied numerically in one dimension. Simulations on the rewired network are performed both in the quenched and in the annealed cases.

For random graphs, studied only at the mean-field level, the probability distribution is assumed to be Poissonian,

$$P(k) = \frac{z^k e^{-z}}{k!},$$

corresponding to drawing Nz links at random among the N nodes ($\mu_2 = z$).

The scale-free network that we study numerically is asymmetric: each node i has a certain number $k_{in}(i)$ of input contacts and $k_{out}(i)$ of output ones, and was grown using the following rule.

We start with a ring of K nodes, and we add the other $N - K$ nodes by choosing, for each of them, K connected nodes j_n , $n = 1, \dots, K$, with probability $k_{in}(j_n) / \sum_{l=1}^N k_{in}(l)$ (preferential attachment). The node being attached is added to the *inputs* of the chosen nodes. We also choose another node at random and add it to the list of input nodes of the new node. This process simulates the growth of a social network in which a new node (a family or an individual) is born from another one (the ones that are added as input of the newborn node) and joins the society according to the popularity of nodes.

Our procedure allows one to generate a network that has a power-law distribution of input contacts, $P_{in}(k) \approx k^{-\gamma}$, with $\gamma \approx 2$ (see Fig. 1), while the distribution of output connections, $P_{out}(k)$, is found to be exponentially distributed. This is an interesting feature of the model as the input connections represent the total number of contacts to which an individual is exposed, while the output connections represent the actively pursued contacts, e.g., familiar ones. A customer, for instance, is exposed to a large number of obliged contacts, and may become infected with a large probability. These are considered “input” links. On the other hand, people in a public position are more monitored, and it is not plausible that they can infect a comparably large number of people. Infection is limited to the private sphere, where contacts are more

intense. These are the “output” links. We choose this algorithm in order to have a “worst-case” scenario, with an exponent corresponding to a diverging average of input connectivity.

We have not studied the case of dynamic dependence of the network on the infection level, however, a high level of infection of a severe disease may surely induce changes in the social network. It is reasonable to assume that, for mild diseases (or diseases considered harmless, like most computer viruses), the social network is not affected and only the level of prevention is increased.

In the present paper we assume the effects of the infection to be immediately visible, with no latency or “hidden infectivity.” We also assume as a temporal unit the time required to recover from an illness without immunization and thus we explore the case of a SIS dynamics.

An individual can be infected separately by each of his neighbors with a probability τ per unit of time [see Eq. (1)]. We model the effects of the perception of the risk of being infected replacing the bare infection probability τ with $\tau I(s, k)$.

$$I(s, k) = \exp\left\{-\left[H + J\left(\frac{s}{k}\right)^\alpha\right]\right\}, \quad (2)$$

where k is the number of neighbors of a given site and s is the number of them that are ill.

We assume the perception of the risk of being infected to depend on the fraction of infected individuals among the neighbors s/k , on the level of precaution measures adopted, J , and on the use of special prophylaxis, $\alpha \leq 1$. The quantity H models a global influence over the population, alarm of broadcasting media news, in which case it could depend on the average level of the infection. Its effect is that of reducing the bare infectivity τ , so in the following we only consider the case $H=0$. For the moment, we consider $\alpha=1$; the role of this parameter will be clear in the following. Differently from Ref. [17], in our model the infectivity is not exclusively related to the connectivity.

A comment about the *linearity* or proportionality of encounters of the source of risk follows. The simplest assumption is that of assuming that the risk of smoking two cigarettes is *twice* that of smoking one cigarette; the risk of exiting two times at night is *double* of going out once, etc.

However, this proportionality can only hold for vanishing probabilities. Actually, probabilities of subsequent independent events factorize. So, assuming that there is a given probability p of smoking a cigarette, and that an advertisement has an effect a on stopping this habit, then the probability of smoking after having received one alert is $p(1-a)$, after having received two alerts is $p(1-a)^2$, and after n alerts is $p(1-a)^n \approx p \exp(-an)$, which is the motivation of Eq. (2).

The mean-field return map (for fixed connectivity z) is shown in Fig. 2. The effect of the introduction of risk perception is evident: for high concentrations of infected individuals the probability of being infected is diminished. Therefore, while for $J=0$ and $z>1$ there is only one stable

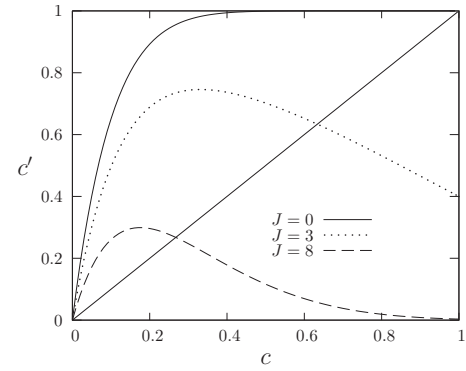


FIG. 2. Mean-field return map for fixed connectivity $z=10$, parameters $H=0$, $\alpha=1$, $\tau=1$, and varying values of precaution level J . The effect of risk perception (J) is to lower the infectivity at high concentrations of infected individuals.

fixed point $c=1$ (all individuals infected), by increasing J one can have stable fixed points $c < 1$, limit cycles, and even chaotic behavior [29].

III. MEAN-FIELD ANALYSIS

The simplest mean-field approximation of the evolution of disease on a network consists of neglecting correlations among variables. This is essentially equivalent in considering the evolution on a tree, i.e., in assuming the absence of loops.

Let us denote with $c_k=c_k(t)$ the probability of having an infected site of degree k (with k connections) at time t , and with $c'_k=c_k(t+1)$, the probability at a subsequent time step.

The mean evolution of the system is generically given by

$$c'_k = \sum_{C_k} P_C(k|C_k) P_I(k, C_k) P_H(C_k),$$

where C_k indicates the local configuration (degrees and healthy status) at time t around a site of degree k . $P_H(C_k)$ is the probability of occurrence of the healthy status of such a configuration, $P_C(k|C_k)$ is the probability that the local configuration is connected to the site under examination, and $P_I(k, C_k)$ is the probability that the disease propagates in one time step from C_k to the site.

In our case, the local configuration is given by a set of k nodes, of degree (n_1, n_2, \dots, n_k) , and status (s_1, s_2, \dots, s_k) , where $s_i=0$ (1) indicates that the site i is healthy (ill). Thus $C_k=(n_i, s_i)_{i=1}^k$ and $P_H(C_k)=\prod_{i=1}^k c_{n_i}^{s_i} (1-c_{n_i})^{1-s_i}$ since we assume decorrelation among sites.

$P_C(k|C_k)$ depends on the assortativity of the network. Let us define $P_L(n|k)$ as the probability that a site of degree k is attached to a link connected to a site of degree n . $P_L(n|k)$ is computed in an existing network as the number of links that connects sites of degree n and k , divided by the total number of links that are connected to sites of degree k , and $\sum_n P_L(n|k)=1$. The detailed balance condition gives $kP_L(n|k)P(k)=nP_L(k|n)P(n)$. For nonassortative networks, $P_L(n|k)=\phi(n)$, and summing over the detailed balance condition one gets $P_L(n|k)=nP(n)/z$, where z is the average

number of links per node, $z = \sum_k k P(k)$. Assuming again a decorrelated network, we have

$$P_C(k|C_k) = \prod_{i=1}^k P_L(n_i|k) = \prod_{i=1}^k \frac{n_i P(n_i)}{z}$$

for nonassortative networks.

$P_I(k, C_k)$ is the infection probability. In the case without risk perception, it is

$$P_I(k, C_k) = [1 - (1 - \tau)^s],$$

where $s = \sum_i s_i$. The risk perception is modeled by replacing τ with $\tau \exp(-Js/k)$, which makes the equations hard to be managed analytically except in the limit of vanishing infection probability $c_k \rightarrow 0$, for which only the case $s=1$ is relevant. We shall consider this point later.

Put all together, one gets

$$c'_k = \sum_{n_1, n_2, \dots, n_k} \left[\prod_{i=1}^k P_L(n_i|k) c_{n_i}^{s_i} (1 - c_{n_i})^{1-s_i} \right] \left[1 - \prod_i (1 - \tau)^{s_i} \right].$$

Using the relation

$$\sum_{x_1, x_2, \dots, x_k} \prod_i f(x_i) = \left(\sum_x f(x) \right)^k,$$

we obtain after some simplifications,

$$c'_k = 1 - \left[1 - \tau \sum_n c_n P_L(n|k) \right]^k.$$

This expression could be obtained directly by noticing that $1-c$ is the probability of not being ill, which corresponds to the combined probability of not being infected by any of the k neighbors. Neglecting correlations, these are k independent processes (although they depend on k). Each of these processes is 1 minus the probability of being infected, which is the sum, over all possible degree n of the neighboring node, of the probability that it is ill (c_n) times the probability that it is connected to the node under investigation, $P_L(n|k)$.

Let us denote by \bar{c} the asymptotic value of $c(t)$. Assuming that the transition between the quiescent ($\bar{c}=0$) and active ($\bar{c}>0$) is continuous, its boundary is given by the values of parameters for which $c'/c=1$ in the limit $c \rightarrow 0$. In this limit

$$c'_k \simeq k\tau \sum_n c_n P(n|k),$$

and we can now consider the case with risk perception, with τ replaced by $\tau \exp(-J/k^\alpha)$.

In the case of nonassortative networks,

$$c_k(t+1) = k \frac{\tau}{z} \exp\left(-\frac{J}{k^\alpha}\right) \sum_n c_n(t) n P(n).$$

Calling $a(t+1) = \sum_n c_n(t) n P(n)$ (that does not depend on k), we have $c_k(t) = (k\tau)/z \exp(-J/k^\alpha) a(t)$ and thus

$$c_k(t+1) = c_k(t) \frac{\tau}{z} \sum_n \exp\left(-\frac{J}{n^\alpha}\right) n^2 P(n).$$

The critical boundary is therefore given by

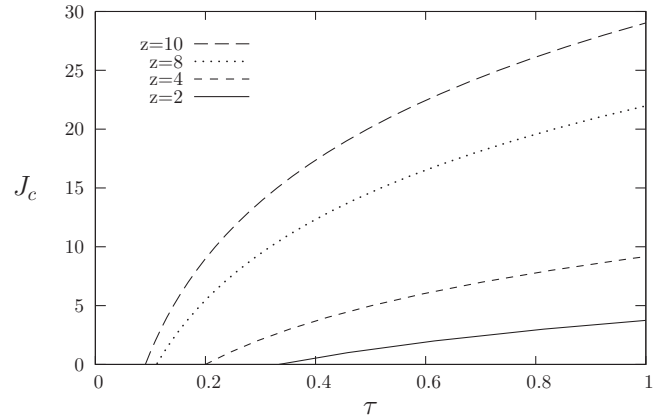


FIG. 3. The mean-field dependence of the critical value of precaution level J_c , with respect to the bare infectivity τ for Poissonian networks, with average connectivity z and $\alpha=1$.

$$\sum_k \exp\left(-\frac{J_c}{k^\alpha}\right) k^2 P(k) = \frac{z}{\tau}, \quad (3)$$

from which one could obtain J_c as a function of τ (we replaced n by k for consistency with the rest of the paper). In the case $J=0$ (no risk perception), the formula gives

$$\tau_c = \frac{\mu_2}{z} = \frac{\langle k^2 \rangle}{\langle k \rangle},$$

which is a well-known result [9,16].

In the case of fixed connectivity, $P(k) = \delta_{kz}$, and for $\alpha=1$,

$$J_c = z \ln(\tau z). \quad (4)$$

In the absence of perception ($J=0$) one has $\tau_c = 1/z$.

For Poissonian networks (random graphs),

$$P(k) \simeq \frac{z^k e^{-z}}{k!}.$$

Numerical integration of Eq. (3) for $\alpha=1$ gives the results shown in Fig. 3. One can notice that for every value of τ and finite average connectivity z , there is always a value of the precaution level J_c that leads to the extinction of the epidemics.

For nonassortative scale-free networks with exponent γ , $P(n) \propto n^{-\gamma}$, the sum in Eq. (3) diverges unless $\gamma > 3$, irrespective of α .

This implies that at the mean-field level, any level of precaution is not sufficient to extinguish the epidemics.

IV. NUMERICAL RESULTS

The mean-field approximation disregards the effects of (correlated) fluctuations in the real system. Indeed, the effects of random and/or long-range connections may disrupt correlations. We found that the behavior of microscopic simulations with random rewiring, both in the quenched and annealed version, is well reproduced by mean-field simulations with a white noise term, with amplitude proportional to $\sqrt{c(1-c)N}$. The noise term (or the fluctuations in micro-

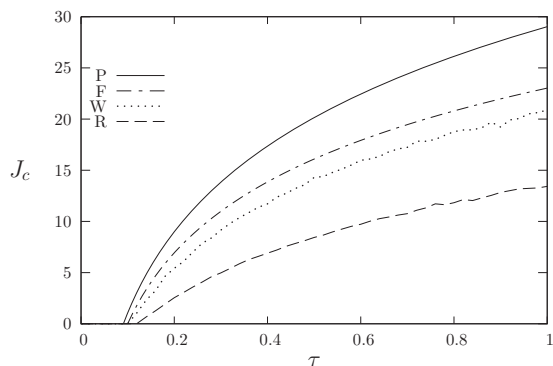


FIG. 4. Critical value J_c of the precaution level as a function of the base infectivity τ average connectivity $k=10$ for the Poissonian mean-field (P), fixed connectivity mean field, Eq. (4) (F), and numerically ($N=1000$), for the annealed rewired $p=1$ (W), and regular one-dimensional (R) cases.

scopic simulations) may bring the infection to extinction if the average (or mean-field) oscillations come close to $c=0$, as is often the case for a choice of J for which chaotic behavior appears in the mean-field approximation.

For regular (fraction of rewired links $p=0$) and rewired ($p>0$) lattices, it is always possible to observe a continuous transition toward a critical level $J_c(\tau)$, such that the infection becomes extinct, for every value of the bare infectivity τ , as shown in Fig. 4.

For scale-free networks, we concentrated on the case illustrated in Sec. II, which can be considered a worst-case scenario ($\gamma=2$, diverging second and first moments of input distribution).

Simulations show that for $\alpha=1$ [Eq. (2)], there is no value of J_c for which the infection may be stopped (although not all population is always infected), for any value of τ , in agreement with the mean-field analysis.

The investigation of nodes that are *more responsible* for the spreading of the infection reveals, as expected, that the nodes with higher input connectivity (hubs) stay ill most of the time (Fig. 5). Notice that also nodes with high input connectivity have finite output connectivity, so the above relation is not trivially related to the infection level.

In real life, however, public service workers who are exposed to many contacts (such as medical doctors, for instance) use additional safety measures. In order to include this effect in the model, we use the parameter α , Eq. (2), that

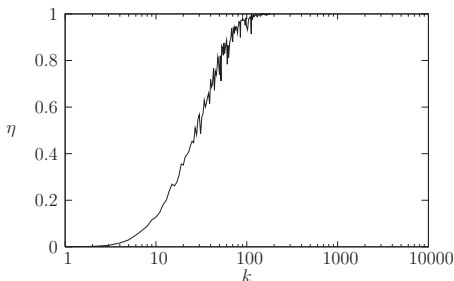


FIG. 5. Fraction of time spent ill (η) in the scale-free case, as a function of k for $K=10$, $J=10$.

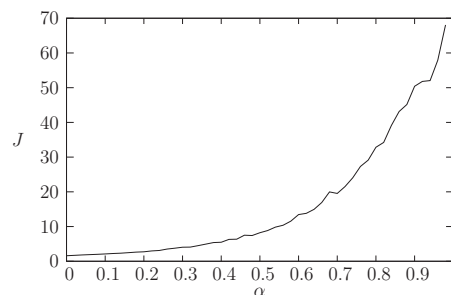


FIG. 6. Dependence of the critical value of the perception J_c , as a function of the *exposure-enhanced* perception parameter α , $K=4$, $\tau=1$, $N=10\,000$.

up to now has been set to one. The effect of this parameter is to increase the perception of the risk (or the safety measures) for nodes with higher connectivity. As shown in Fig. 6, as soon as $\alpha < 1$, a finite critical value of J_c appears. The transition from the active ($c>0$) state to the absorbing ($c=0$) state occurs suddenly, due to fluctuations. Essentially, nodes with high connectivity may fail to be infected due to their increased perception of the infection, and this efficiently stops the spreading. This effect is similar to targeted immunization, but is not captured by the mean-field analysis. It is a dynamical effect over a network far from the percolation threshold, and thus contains loops.

The transition may be a finite-size effect, related to the unavoidable cutoff in the degree distribution for finite populations, although simulations with populations from $N=5000$ up to $N=80\,000$ do not show any systematic change in the transition point.

V. CONCLUSIONS

In conclusion, we have studied the effects of risk perception in a simple SIS model for epidemics spreading. These effects are modulated by two parameters J and α , which reduce the infectivity of the disease as a function of the fraction of people in the neighborhood that are manifestly ill. The first parameter modulates the linear response, while the second models nonlinear effects such as the increase of prevention due to a publically exposed role. We found that for fixed or peaked connectivity there is always a finite value J_c of perception that makes the epidemics go extinct. We studied the evolution of the disease in a “worst-case” social network, with scale-free input connectivity and an exponent $\gamma \approx 2$, for which both the average input connectivity and fluctuations diverge. In this case a linear perception cannot stop the disease, but we found that, as soon as the perception is increased in a nonlinear way ($\alpha < 1$), the epidemics may become extinct by increasing the perception level. This latter transition is not continuous and is presumably induced by fluctuations in hubs. It may be due to the finiteness of population. Notice that, for a given local infection level s , the infectivity in our model increases with the connectivity k , differently from what happens in other models.

The mechanism that we propose is somehow analogous to vaccination of hubs, except that it is a dynamics effect due to

the local level of diffusion of the disease, and is not exclusively related to local connectivity. We think that a similar mechanism is at the basis of the robustness of human population with respect to epidemics, even in the absence of immunization procedures. One may speculate that, as a consequence of such robustness, humans have been selected to exhibit visual signs of the most common diseases, which certainly does not favor the spread of infective agents. An-

other common symptom of an illness is the tendency to isolation, which again could be the result of selection.

ACKNOWLEDGMENTS

L.S. research is supported by the EMBO organization under Contract No. ASTF 12-2007. The authors acknowledge fruitful discussions with F. Di Patti and A. Guazzini.

-
- [1] V. Colizza, A. Barrat, M. Barthélemy, and A. Vespignani, Proc. Natl. Acad. Sci. U.S.A. **103**, 2015 (2006).
- [2] D. J. Watts and S. H. Strogatz, Nature (London) **393**, 440 (1998).
- [3] R. Pastor-Satorras and A. Vespignani, Phys. Rev. E **63**, 066117 (2001).
- [4] M. E. J. Newman, SIAM Rev. **45**, 167 (2003).
- [5] R. Albert and A.-L. Barabasi, Rev. Mod. Phys. **74**, 47 (2002).
- [6] S. N. Dorogovtsev, J. F. F. Mendes, and A. N. Samukhin, Phys. Rev. Lett. **85**, 4633 (2000).
- [7] In SIR dynamics the infective node cannot be reinfected, so k is replaced by $k-1$.
- [8] R. M. Anderson and R. M. May, *Infectious Diseases of Humans: Dynamics and Control* (Oxford University Press, Oxford, 1991).
- [9] M. Boguñá, R. Pastor-Satorras, and A. Vespignani, Phys. Rev. Lett. **90**, 028701 (2003).
- [10] A. Vázquez and Y. Moreno, Phys. Rev. E **67**, 015101(R) (2003).
- [11] Y. Moreno, J. B. Gómez, and A. F. Pacheco, Phys. Rev. E **68**, 035103(R) (2003).
- [12] V. M. Eguiluz and K. Klemm, Phys. Rev. Lett. **89**, 108701 (2002).
- [13] A. Vázquez, M. Boguna, Y. Moreno, R. Pastor-Satorras, and A. Vespignani, Phys. Rev. E **67**, 046111 (2003).
- [14] R. Cohen, S. Havlin, and D. ben-Avraham, Phys. Rev. Lett. **91**, 247901 (2003).
- [15] R. D. Smith, *Infectious Disease and Risk: Lessons from SARS* (The Nuffield Trust, London, 2005).
- [16] M. E. J. Newman, Phys. Rev. E **66**, 016128 (2002).
- [17] R. Olinky and L. Stone, Phys. Rev. E **70**, 030902(R) (2004).
- [18] D. S. Callaway, M. E. J. Newman, S. H. Strogatz, and D. J. Watts, Phys. Rev. Lett. **85**, 5468 (2000).
- [19] R. Cohen, K. Erez, D. ben-Avraham, and S. Havlin, Phys. Rev. Lett. **85**, 4626 (2000).
- [20] S. Riley *et al.*, Science **300**, 1961 (2003).
- [21] M. Lipsitch *et al.*, Science **300**, 1966 (2003).
- [22] L. Hufnagel, D. Brockmann, and T. Geisel, Proc. Natl. Acad. Sci. U.S.A. **101**, 15124 (2004).
- [23] M. Kamo and A. Sasaki, Physica D. **165**, 228 (2002).
- [24] R. Pastor-Satorras and A. Vespignani, Phys. Rev. Lett. **86**, 3200 (2001).
- [25] A. H. Eagly and S. Chaiken, *The Psychology of Attitudes* (Harcourt, Fort Worth, TX, 1993); A. H. Eagly and S. Chaiken, "Attitude Structure and Function," in *The Handbook of Social Psychology*, edited by D. T. Gilbert, S. T. Fiske, and G. Lindzey (McGraw-Hill, New York, 1998), Vol. 1, pp. 269–322; S. T. Fiske and S. L. Neuberg, "A Continuum of Impression Formation, from Category-Based to Individuating Processes: Influences of Information and Motivation on Attention and Interpretation," in *Advances in Experimental Social Psychology*, edited by M. P. Zanna (Academic Press, New York, 1990), Vol. 23, pp. 1–74.
- [26] P. Glendinning and L. P. Perry, J. Math. Biol. **35**, 359 (1997).
- [27] B. T. Grenfell, O. N. Bjørnstad, and B. F. Finkenstädt, Ecol. Monogr. **72**, 185 (2002).
- [28] N. T. J. Biley, *The Mathematical Theory of Infectious Diseases and its Applications*, 2nd ed. (Griffin, London, 1975); J. D. Murray, *Mathematical Biology: I. An Introduction*, 3rd ed. (Springer, Berlin, 2002).
- [29] L. Sguanci, P. Lió, and F. Bagnoli, "The Influence of Risk Perception in Epidemics: A Cellular Agent Model," in *Cellular Automata*, edited by S. El Yacoubi, B. Chopard, and S. Bandini, Lecture Notes in Computer Science Vol. 4173 (Springer, Berlin, 2006), pp. 321–329.
- [30] N. Boccaro, O. Roblin, and M. Roger, Phys. Rev. E **50**, 4531 (1994).
- [31] F. Bagnoli, F. Franci, and R. Rechtman, Phys. Rev. E **71**, 046108 (2005).